DOI: 10.1016/S1872-5805(21)60072-0

Recent advances in carbon-supported iron group electrocatalysts for the oxygen reduction reaction

LI Ping, WANG Huan-lei*

(*School of Materials Science and Engineering*, *Ocean University of China*, *Qingdao* 266100, *China*)

Abstract: Metal-air batteries are emerging energy devices that have received worldwide attention. The oxygen reduction reaction (ORR) is the key electrochemical process of metal-air batteries. The sluggish nature of ORR kinetics and the high cost of Pt-based ORR catalysts have severely hindered their large-scale application. As earth-abundant elements, the iron group elements have a variety of hybrid orbitals, and their incorporation into the carbon skeleton achieves good ORR catalytic activity, giving them great potential for substituting for Pt-based catalysts. Here, their uses for ORR and the function of each active site in the ORR process are summarized. The relationship between the microstructure and performance of these catalysts may help us fully understand the role of iron group elements in ORR and provide basic insight into the design of cheap catalysts with outstanding ORR catalytic performance in the future.

Key words: Iron series elements; Carbon electrocatalysts; Heteroatomic doping; Oxygen reduction reaction; Adjustment and control of structure

1 Introduction

With the increasing demand for addressing the global environmental and energy problems by utilizing clean energy, metal-air batteries are considered to be one of the effective technologies for solving this issue[1]. In metal-air batteries, the chemical energy can be directly converted into electrical energy, and this process does not need combustion and is not limited by Carnot cycle, thus improving energy conversion efficiency and reducing unnecessary energy loss[2]. Metal-air batteries demonstrate the merits of low cost, safety, environmental friendliness and high theoretical energy density. Metal-air batteries consist of a metal as an anode and air as a cathode. In general, the oxygen reduction reaction (ORR) process on the cathode of metal-air batteries mostly displays complex and low reaction rate in alkaline media[3, 4], which is the main obstacle hindering the large-scale application of metal-air batteries[5]. The development of high-efficiency catalysts is the main task for boosting the ORR process. The precious Pt metal shows the best catalytic performance. However, the large-scale application of metal-air batteries is limited by the high cost and low reserve of Pt[6]. The preparation of cheap and high-performance ORR catalysts to replace precious metals still remains a big challenge. During the past decades, carbon-based catalysts with the advantages associated with high surface area, low-cost, outstanding conductivity, and stable physicochemical stability have been extensively investigated to enhance the sluggish ORR process. The electronic environment of the carbon catalysts can be modulated by introducing nonmetallic heteroatoms (such as N, P, B, O, etc), and the doping engineering strategy is proved to effectively boost the ORR catalytic performance. However, compared with Pt, there is still a performance gap for carbon-based catalysts. Based on the characteristics of abundant reserves, low price, low biological toxicity, and similar physicochemical property for transition metals, introducing iron, cobalt and nickel (called iron series elements) based active species into carbon-based catalysts is an insightful idea to realize the preparation of high-performance ORR catalysts[7].

Iron series elements with unique electronic structure and low crystal field splitting energy are facile for forming metal complexes with weak field ligands (such as ligands with P and N as coordination atoms)[8, 9]. High spin iron series complexes can also

Received date: 2021-06-02; **Revised date:** 2021-06-27
Corresponding author: WANG Huan-lei, Professor. E-mail: huanleiwang@ouc.edu.cn
Author introduction: LI Ping, Ph.D candidate. E-mail: chemlipingest@163.com

change the spin state through spin crossover, resulting in the reduction of the reaction energy barrier for promoting the ORR reaction. As a result, it is the potential direction of research to replace precious metals with cheap and abundant transition metals as ORR catalysts. In recent years, iron series compounds, such as oxides, chalcogenides, carbides, phosphates and nitrides, have been incorporated within carbon matrix as high-performance ORR catalysts[10–12]. The introduction of carbon matrix can not only provide excellent conductivity framework, but also avoid the agglomeration of iron series compounds[13]. At the same time, iron series elements can change the electronegativity of carbon to improve the catalytic activity of the materials[14]. Besides, for further optimizing the intrinsic activity of iron series compounds, determining their ORR activity is necessary[15–17]. Although iron series elements based carbon catalysts show excellent catalytic activity, the reason of catalytic performance improvement should be clearly clarified. Therefore, it is crucial to give timely summarization on this field for emphasizing the origin of internal activities.

Therefore, in this review, we discuss the application of iron series compounds in ORR catalysts according to the classification of active sites (Fig. 1). For clearly, the active sites are clarified as M-N_x, M-P_x, M-O_x, M-S_x, M-C_x and metal nanoparticles. The different active centers and catalytic mechanisms of the iron catalysts were thoroughly discussed. For better designing ORR catalysts with high catalytic performance, we systematically elucidate the relationship between the microstructure and performance of carbon-supported catalysts based on iron series elements.

2 General principles of ORR

The ORR reaction is a multi-electron reaction, and the whole reaction process can be simply divided into $4e^-$ pathway and $2e^-$ pathway[29, 30]. The $4e^-$ process with high energy conversion rate and output voltage is an ideal reaction way for oxygen reduction in cathodes in metal-air batteries[31]. High $4e^-$ path selectivity is a major parameter for evaluating ORR catalysts. The conversion of O_2 to H_2O via $4e^-$ pathway is the optimum way (eqn (1-5))[32]:

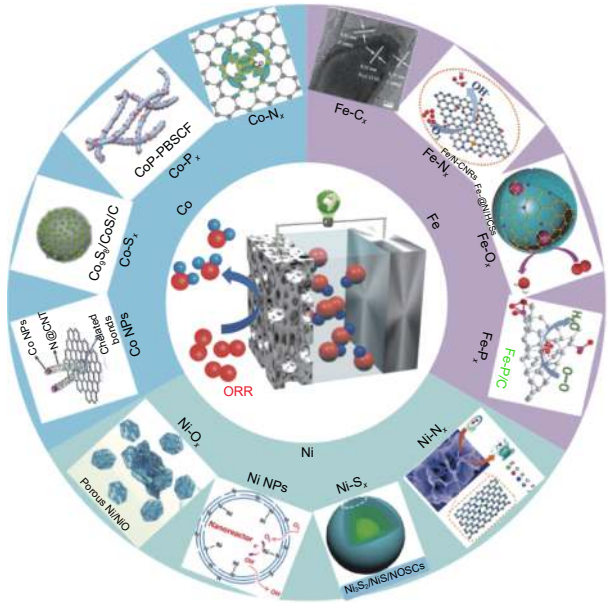

Fig. 1 Summary of carbon-supported iron series element catalysts in ORR, such as Fe-N_x (Reprinted with permission by copyright 2021, Willey[16]), Fe-O_x (Reprinted with permission by copyright 2020, Willey[18]), Fe-P_x (Reprinted with permission by copyright 2020, ACS[19]), Ni-N_x (Reprinted with permission by copyright 2020, RSC[20]), Ni-S_x (Reprinted with permission by copyright 2018, ACS[21]), Ni NPs (Reprinted with permission by copyright 2017, Willey[22]), Ni-O_x (Reprinted with permission by copyright 2020, Springer Nature[23]), Co NPs (Reprinted with permission by copyright 2020, Willey[24]), Co-S_x (Reprinted with permission by copyright 2019, Willey[25]), Co-P_x (Reprinted with permission by copyright 2019, RSC[26]), Co-N_x (Reprinted with permission by copyright 2020, Willey[27]) and Fe-C_x (Reprinted with permission by copyright 2020, Elsevier[28]).

$$O_2 + * \rightarrow O_2^* \quad (1)$$

$$O_2^* + H_2O + e^- \rightarrow OOH^* + OH^- \quad (2)$$

$$OOH^* + e^- \rightarrow O^* + OH^- \quad (3)$$

$$O^* + H_2O + e^- \rightarrow OH^* + OH^- \quad (4)$$

$$OH^* + e^- \rightarrow OH^- + * \quad (5)$$

Where the * represents the active site of the catalyst, and the OOH*, O* and OH* are intermediates produced in ORR process. The formation of OOH* is a rate-limiting step, and the real reaction mechanism of $4e^-$ process is mainly determined by the dissociation energy of O_2 on the electrocatalyst.

3 Different carbon carriers in ORR catalysts

The application of metal elements in ORR catalysts may face the problems of poor dispersion, low utilization and poor conductivity. The optimal way to solve this problem is to introduce carbon carriers. Car-

bon-based supports with porous, two-dimensional, and/or fibrous structures can improve the mass/electron transport ability and allow more accessible active sites. Among the different carbon nanomaterials, carbon nanotubes, graphene and porous carbon materials are extensively used in the field of electrocatalysis. In the two-dimensional graphene, the active catalytic components can be arranged in different ways, such as horizontally or vertically dispersed in the surface, assembled into clusters, or completely filled in the interlayer space[33]. Similar to graphene, carbon nanotubes has the advantages associated with intrinsic sp^2 hybrid structure, excellent conductivity, and good chemical stability[34, 35]. Therefore, carbon nanotubes are also considered as promising carriers for preparing electrocatalysts[36]. However, metal active species loaded onto the carbon nanotubes can be easily agglomerated. Moreover, graphene and carbon nanotubes are easy to stack and agglomerate, so it is necessary to build the 3D network by using graphene or carbon nanotube blocks. Porous carbon with high surface area and developed porosity, which provides abundant active sites for anchoring metal species and affords a large number of transport channels[37]. The controllable porous structure of porous carbon can prevent the aggregation of metal active sites during the catalytic process, thus extending the life of the catalyst. Besides, other carbon materials, such as carbon cloth, carbon fibers, and activated carbons, can be also used as supports in the electrocatalysts. The interaction between pure carbon carriers and metal sites is very weak and usually requires the introduction of heteroatoms or functional groups[38]. This can not only enhance the interaction between carbon carriers and metal active sites, but also provide additional nonmetal active sites, thus improving the cycling stability and catalytic activity of the catalyst.

4　Carbon-supported M-N_x-based catalysts for ORR

When the iron series metal atoms bond with nitrogen atoms, the *d*-band structure of the host metal can be shrunk, fundamentally regulating the activity of the catalytic site[39]. When the d_z^2 orbital of a metal is empty, the adsorption of oxygen atom on the metal and the transfer of electrons from the metal to the anti-π* orbital of O to form the metal-oxygen chelated intermediate can be accelerated[40]. Therefore, in the catalytic reaction of oxygen reduction, (Fe,Co,Ni)-N_x based catalysts show strong oxygen adsorption strength, indicating the great potential for cathodic oxygen reduction catalysts[41]. Moreover, due to the Pt-like electronic structure, the theoretical electrocatalytic activity of (Fe,Co,Ni)-N_x based catalysts is similar to that of Pt.

Due to the hybridization between N 2*p* and M 3*d*, M-N_x is considered to be the active site for ORR, especially Fe-N_4 with a planar structure[42]. In principle, the active site associated with Fe-N_x have five possible coordination numbers, and the coordination number *x* can significantly affect the charge distribution of metal sites, resulting in the change of catalytic performance of Fe-N-C. The optimal adsorption configurations of ORR intermediates O*, OH* and OOH* on Fe-N_x (x = 1-5) were predicted by theoretical calculation[43, 44]. Theoretically, the order of ORR activity is Fe-N_4>Fe-N_3>Fe-N_2>Fe-N_1>Fe-N_5[45]. As a result, Fe-N_4 shows the best activity, and OH*/H_2O can be easily adsorbed/desorbed on/from Fe-N_4. Fe-N_4 not only acts as an effective active site, but also promotes ORR reaction by changing the surrounding carbons from electron rich to electron deficient[43], and this regulation of electronic structure of carbon is prone to obtain a high ORR initial potential[46]. Shao et al. prepared petal-like porous carbon nanosheets with Fe-N_4 species (FeNC-D0.5) by utilizing the space limitation of silica with the coordination of diethylenetriaminepentaacetic acid (DTPA) and melamine (Fig. 2a)[47]. The half-wave potential ($E_{1/2}$) of FeNC-D0.5 is 0.866 V, superior to that of Pt/C (0.845 V). Due to the hard coordination of DTPA and the binding effect of silica, the wrapped Fe atoms can be efficiently isolated for obtaining dense Fe-N_4 site. On the other hand, the petal-like porous structure is beneficial for exposing abundant active centers, leading to the improved ORR catalytic activity of FeNC-D0.5. Furthermore, the ORR activity of FeN_x can be effectively improved by manufacturing defects near FeN_x.

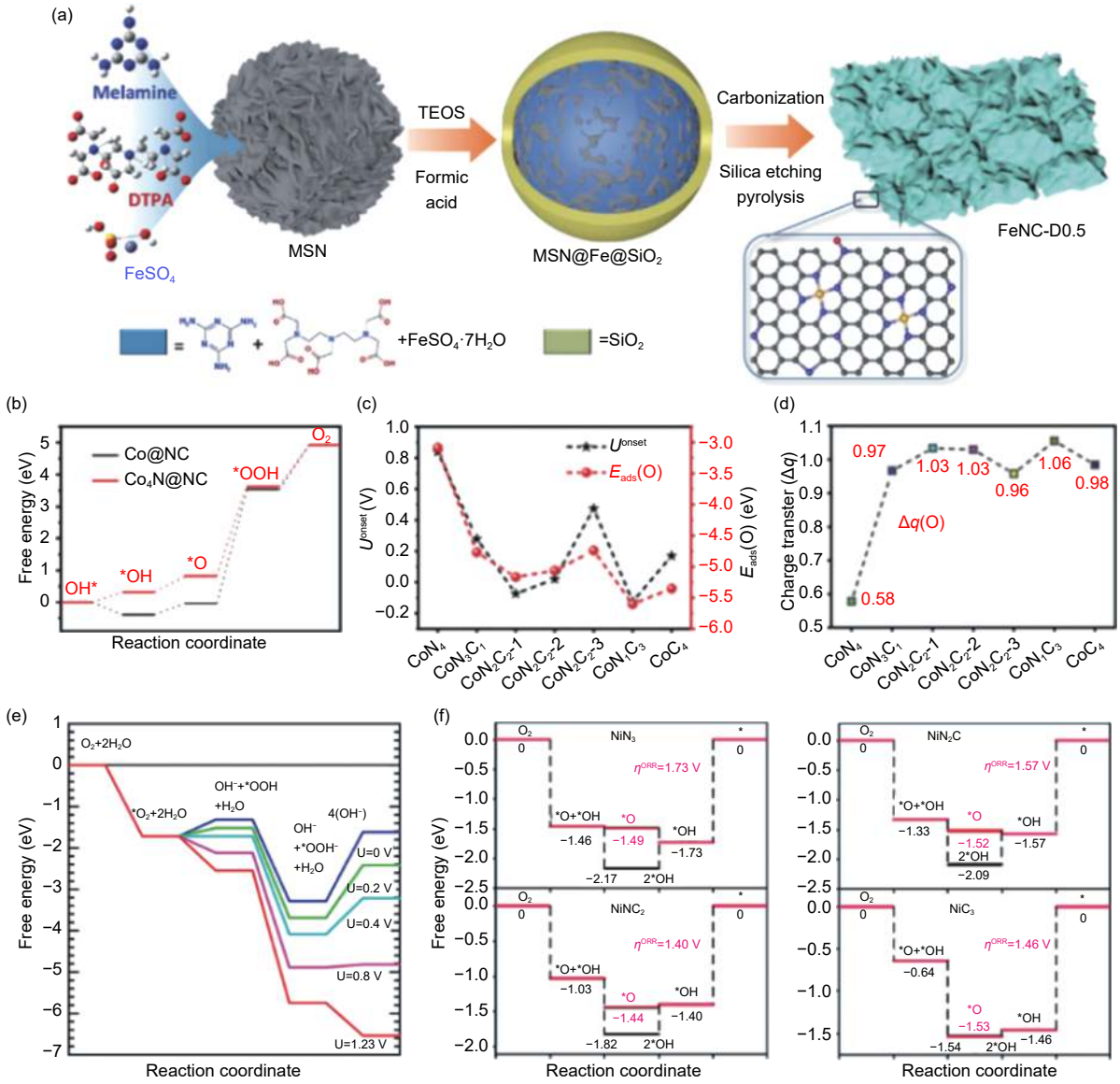

Fig. 2 (a) The synthesis procedure of FeNC-D0.5 (Reprinted with permission by copyright 2021, Willey[47]), (b) the energetic pathway of the ORR on Co_4N@NC (Reprinted with permission by copyright 2020, Elsevier[49]), (c) the correlation between the onset potential (U^{onset}) and adsorption energy (E_{ads}) of the adsorptive oxygen atoms on $CoN_{4-x}C_x$, (d) the Bader charge transfer of the adsorptive oxygen on $CoN_{4-x}C_x$ sites (Reprinted with permission by copyright 2020, Willey[27]), (e) free energy diagram for O_2 reduction on Ni–N_2 edge defect (Reprinted with permission by copyright 2012, ACS[50]) and (f) free energy diagram for ORR on three-coordinated NiN_3, NiN_2C, $NiNC_2$, NiC_3 at the equilibrium potential (U=0.402 V) in alkaline conditions (Reprinted with permission by copyright 2020, RSC[51]).

Huo et el. reported the synthesis of atom dispersed Fe site anchored on porous carbon skeleton (Fe-SA/PC) through a simple dual-confinement route[48]. The Fe-SA/PC shows the $E_{1/2}$ of 0.91 V, suggesting excellent ORR catalytic performance. The spatial restriction effect of micro/mesopores on carbon matrix can effectively inhibit the accumulation of iron and promote the generation of Fe-N_x moieties in the synthetic process. The produced 2D carbon structure with continuous rich mass transport channels and large surface area can be beneficial for the exposure of Fe-N_4 active center, and the adsorption of intermediate products. Density functional theory (DFT) calculations also illustrate that the pore defects near the Fe-N_x species can regulate the electronic structure to optimize the adsorption ability of oxygen intermediates, facilitating for achieving superior electrocatalytic activity.

The research of the Co-N_x electrocatalysts began as early as 1964[52]. Jasinski proved that the Co-coordinated N_4 phthalocyanine complex has excellent

ORR performance in alkaline media. As an important ORR active site, Co-N_x has been widely studied. Direct pyrolysis of the mixture of nitrogen-containing precursor and cobalt salt is a commonly used method to prepare catalysts with Co-N_x active sites[53]. However, the direct pyrolysis of the Co-containing mixture couldn't achieve well-controlled active sites, and the Co sites can be seriously aggregated, which can hamper the activity for ORR. Metal-organic framework materials with the merits of high surface area and developed porosity have aroused worldwide concerns, which is beneficial for the construction of well-dispersed active sites for ORR process. Ge et al. demonstrated the preparation of Co_4N@NC by the pyrolysis of a ZIF-67 precursor[49]. The Co_4N@NC shows excellent ORR catalytic activity with a high half-wave potential (0.84 V) and onset potential (E_{onset}, 0.93 V). In Co_4N@NC, Co_4N nanoparticles are evenly loaded in carbon box, which immensely enhances the conductivity of material and restrains the gather of Co_4N nanoparticles. DFT calculation shows that doping N into metallic Co can highly reduce the band gap of Co, thus notably reducing the overpotential from OH^* to OH^- in the ORR process (Fig. 2b), which is beneficial for realizing excellent and stable ORR activity. Applications of other coordination numbers of cobalt-rich cobalt nitride in ORR are also being investigated. Shu et al. reported a tannic acid assisted nitridation method for preparing a worm-like nitrogen-doped porous carbon embedded with $Co_{5.47}N$ nanoparticles ($Co_{5.47}N$@N-rGO)[54]. Due to the abundant exposed active sites and the coupling effect between the N-rGO layer and $Co_{5.47}N$ nanoparticles, the $Co_{5.47}N$@N-rGO shows a high ORR catalytic activity. Compared with cobalt-rich cobalt nitride, there are more researches on ORR catalytic performance of cobalt-poor cobalt nitride. Sun et al. utilized a MOF template method for preparing a catalyst with a gallstone-like hierarchical structure and CoN_4 active site[55]. DFT calculation shows that the CoN_4 is highly consistent with the ideal's free-energy pathways in a $4e^-$ ORR process, implying its excellent catalytic activity. Although Co-N_4 is generally regarded as an active site, investigating the catalytic activity of Co with partly coordinated N is still necessary. Yang et al. studied the catalytic activity of Co-N_{4-x}-C_x for ORR in an adjustable coordination environment (Fig. 2c,2d)[27]. By calculating the free energy of ORR, it is found that the order of activity is CoN_4 > CoN_2C_2-3 > CoN_3C_1 > CoC_4 > CoN_2C_2-2 > CoN_2C_2-1 > CoN_1C_3. DFT result provides crucial physical insights into Co-N_{4-x}-C_x active sites with different structures, which can efficiently affect the local electronic structure, thus affecting the adsorption of intermediate products. The coupling effect of N and defects play a crucial role in creating highly active CoN_4 and then enhancing the ORR activity.

Similar to Fe and Co, Ni-N_x-based materials also have excellent ORR catalytic activity. Ni-N_x sites embedded in the carbon matrix are conducive to the adsorption of O_2 and the breakage of O_2 double bond. Kattel et al. used DFT to study the effects of graphitic Ni-N_x(x=2,4) and Ni-N_2 edge defect motifs in Ni-N_x/C on ORR activity[50]. The DFT results show that O_2 and peroxide both chemisorb to Ni-N_2 edge site, but not to graphitic Ni-N_2 and NiN_4 edge sites (Fig. 2e). Cai et al. designs a three-dimensional metal-derived catalyst (Ni-NCNT) with NiN_2 as the main active site, and the uniform distribution of NiN_2 active sites in Ni-NCNT boosts the ORR activity through promoting OH* decomposition process[56]. As shown in Fig. 2f, Liang et al. studied the catalytic activities of a three-coordination Ni–N–C catalyst on graphene matrix for ORR through the DFT calculations[51]. In the case of three-coordinated environment, one vacancy is not enough to accommodate the large radius of Ni atom, which causes Ni atoms to extrude from the graphene plane. The protruded Ni atoms can be beneficial for capturing the oxygen-containing intermediates, and the excessive adsorption of OH* results in the excessive overpotential of ORR. Therefore, the coordination of N and C with Ni has a great influence on the ORR activity, and it is necessary to fine-tune the content of C and N during the catalyst synthesis process. Moreover, Cai et al. prepared a NiN_4-C catalyst by pyrolyzing a mixture of nickel salt and 1-ethyl-3-methylimidazolium dicyanamide (EMIM-dca)[20]. The outstanding ORR catalytic performance of the NiN_4-C catalyst is ascribed to the special structure of single-atom-sized Ni-N_4 sites embedded in 3D hierarchical

carbon. Based on DFT calculation, ORR intermediates tend to be adsorbed on Ni atoms, which indicates that the important active site in the NiN_4-C catalyst is Ni-N_4. The NiN_4-C catalyst has a high $4e^-$ ORR selectivity based on the theoretical and experimental results.

5 Carbon-supported M-P_x-based catalysts for ORR

The lone pair electrons in the 3*p* orbital of phosphorus can cause relatively local concentrated charge density, and the empty 3*d* orbital can accommodate the lone pair electrons in the *p* orbital of oxygen molecule, which helps to improve the activity[57]. In addition, compared with other heteroatoms, P atom has a lower electronegativity and larger covalent radius, and the formed iron series metal phosphides show advantages of high conductivity, low cost and special electronic structure, which are demonstrated to be highly active catalysts for ORR. It is reported that iron series metal phosphates with high phosphorus content show high corrosion resistance, which is due to the enhanced thermodynamic stability of metals in metal phosphates[58]. However, the increase of P content can greatly limit the electronic delocalization of metal atoms, thus hindering the conductivity of a metal, and finally resulting in the decreased catalytic activity[59]. Therefore, balancing the ratio between iron series metals and phosphorus is a key factor for the design of phosphates based on iron series metals, which is important for enhancing the ORR ability without seriously damaging the electrical conductivity.

DFT calculations show that Fe-P bond is beneficial for efficiently activating O_2 molecule and facilitating the subsequent ORR process[63, 64]. At the same time, due to the strong electron-donating ability of P, the charge delocalization of adjacent C is accelerated, thus promoting the adsorption of O_2[65]. In 2015, Singh et al. proposed Fe-P-C as the active site of ORR for the first time[19]. Li et al. synthesized a 3D hybrid carbon composite (Fe/P/$C_{0.5}$-800) with large surface area, abundant mesoporous and microporous structure, and high density planar edge by carbonizing the electrospunned [PVA/H_3PO_4/Fe(AC)$_2$] precursor[66]. Due to the stable Fe-P bond and high structural stability, Fe/P/$C_{0.5}$-800 has excellent electrocatalytic stability. In the Fig. 3a-3b, Chen et al. reported the synthesis of Fe_2P dispersed in a 3D N, P-codoped porous carbon (Fe_2P/NPC) by using a grinding-calcination technique with ZnO as the pore-forming agent[60]. The $E_{1/2}$ and E_{onset} of Fe_2P/NPC are 0.872 and 0.997 V, respectively, indicating the excellent catalytic activity. These results show that the existence of Fe-P bond can promote oxygen reduction, and the large surface area with abundant mesopores can facilitate the exposure of active sites and provide fast mass transfer channels, thus improving the ORR activity.

Cobalt phosphides have been demonstrated to be excellent hydrogen evolution reaction (HER) and oxygen evolution reaction (OER) catalysts[67, 68]. However, few cobalt phosphides have been reported as ORR catalysts. Phosphorus element is more electronegative, so there is a significant electron transfer from cobalt to phosphorous in cobalt phosphides, which is the key factor for the excellent catalytic performance of cobalt phosphides[69]. As shown in Fig. 3c,3d, Liu et al. synthesized an excellent ORR electrocatalyst composed of Co_2P embedded in a Co, N and P multi-doped carbon (Co_2P/CoNPC)[61]. The Co_2P/CoNPC exhibits a remarkable ORR activity with high $E_{1/2}$ of 0.843 V. The excellent ORR catalytic performance of the Co_2P/CoNPC is attributed to the synergistic effect of Co_2P and the multi-heteroatom-doped carbon. The charge density distribution and density of states in Co_2P, Co_nP(n=1.12), CoP and Co were investigated. The charge density distributions and densities of states (DOS) of Co_2P at the Fermi level are higher than that of Co_nP(n=1.12) CoP and Co, indicating that more charge carriers can take part in the electrocatalysis process, which is an important reason for the excellent catalytic performance of Co_2P. However, the exposed crystal plane on the surface of the catalyst can also be an important factor for affecting the catalytic activity of the catalysts. Li et al. synthesized highly monodispersed CoP and Co_2P nanocrystals with consistent size and morphology for ORR[62]. Both the ex-

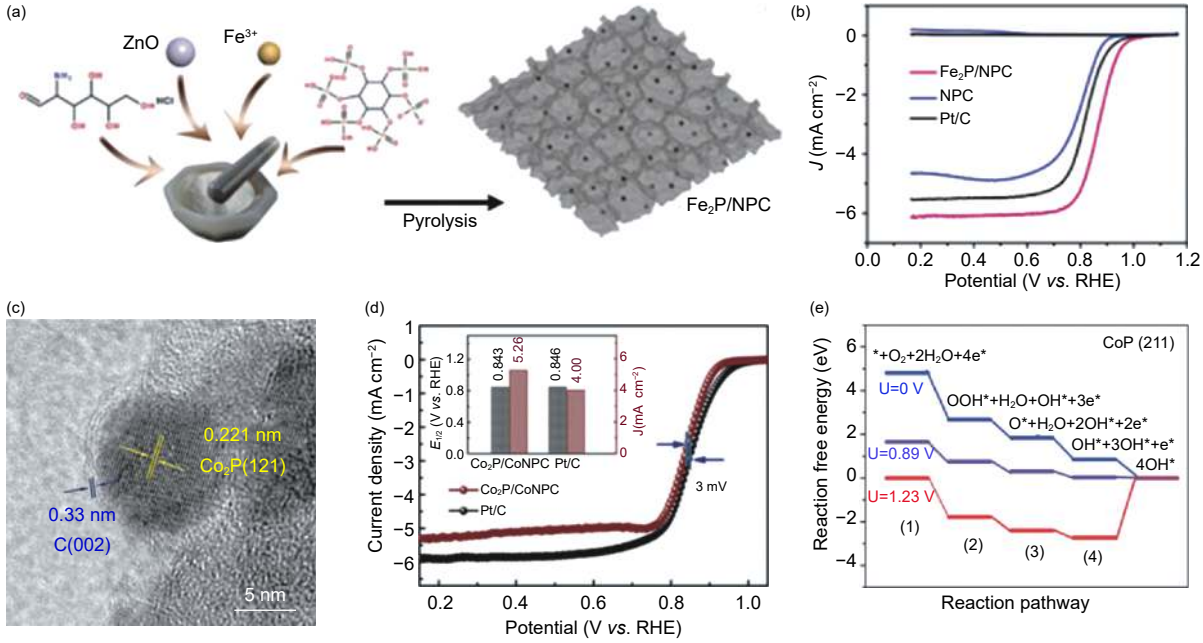

Fig. 3　(a) Schematic illustration of the synthesis for Fe_2P/NPC, (b) rotating ring disk electrode (RRDE) voltammograms of Fe_2P/NPC, NPC, and Pt/C in O_2-saturated 0.10 mol L^{-1} KOH solution (Reprinted with permission by copyright 2020, Elsevier[60]), (c) high resolution-transmission electron microscope (HR-TEM) images of Co_2P/CoNPC, (d) the linear sweep voltammetry (LSV) curves of Co_2P/CoNPC (Reprinted with permission by copyright 2020, Willey[61]) and (e) free energy diagrams for ORR at different electrode potentials on CoP (211) surface through the oxygen associative mechanism (Reprinted with permission by copyright 2018, Willey[62]).

perimental and DFT calculation results show that CoP nanocrystals have more excellent ORR catalytic activity than that of Co_2P due to the highly exposed (211) crystal plane and a large amount of surface phosphide atoms (Fig. 3e). Many other CoP based materials, such as CoP@CC[70], CoP-PBSCF[26], CoP/NP-HPC[71], CoP@SNC[72] and CoP@PNC-DoS[73]) with excellent ORR catalytic activity have been synthesized. Based on these investigations, it is noteworthy that designing catalysts with high surface area and developed pores is vital in the improvement of catalytic performance.

6　Carbon-supported M-O_x-based catalysts for ORR

Iron series metal oxides have received wide attention owing to their low cost, easy availability, unique 3d electronic structure and high surface chemical stability[74]. However, due to the low conductivity and uncontrollable size of iron series metal oxides, the electron transfer and reaction process are seriously hindered, resulting in sluggish reaction kinetics and high polarization[75]. Therefore, it is important to improve the charge transfer ability by combining high conductivity carbon matrix with iron series metal oxides.

As shown in Fig. 4a-c, Wang et al. synthesized ultrafine cobalt oxide nanoparticles loaded on carbon cloth (NP-Co_3O_4/CC), and the NP-Co_3O_4/CC shows excellent ORR activity, showing $E_{1/2}$ of 0.9 V and outstanding ORR durability (Fig. 4a-4c)[76]. Yu et al. synthesized a hierarchical Co_3O_4@N-doped partly-graphitized carbon wrapped by Ti^{3+}-self-doped TiO_2 nanoparticles with multiple crystal-phases as catalysts (Co_3O_4@NGC@MP-TiO_2) for ORR[77]. The possible ORR mechanism on Co_3O_4@NGC@MP-TiO_2 is shown in Fig. 4d. The Co^{2+} can coordinate with the O atom of H_2O, and the H atoms of H_2O can be distributed over the surface of Co_3O_4@NGC@MP-TiO_2. Co^{2+}–OH^- species can be formed due to the reduction of the charge compensation for boosting the protonation of surface oxygen ligands with the existence of Co^{2+}. Du et al. prepared the highly stable and active ORR catalysts (Co_3O_4@NGC@CuO) from the carbonization of ZIF-67 with coating of CuO[78]. The

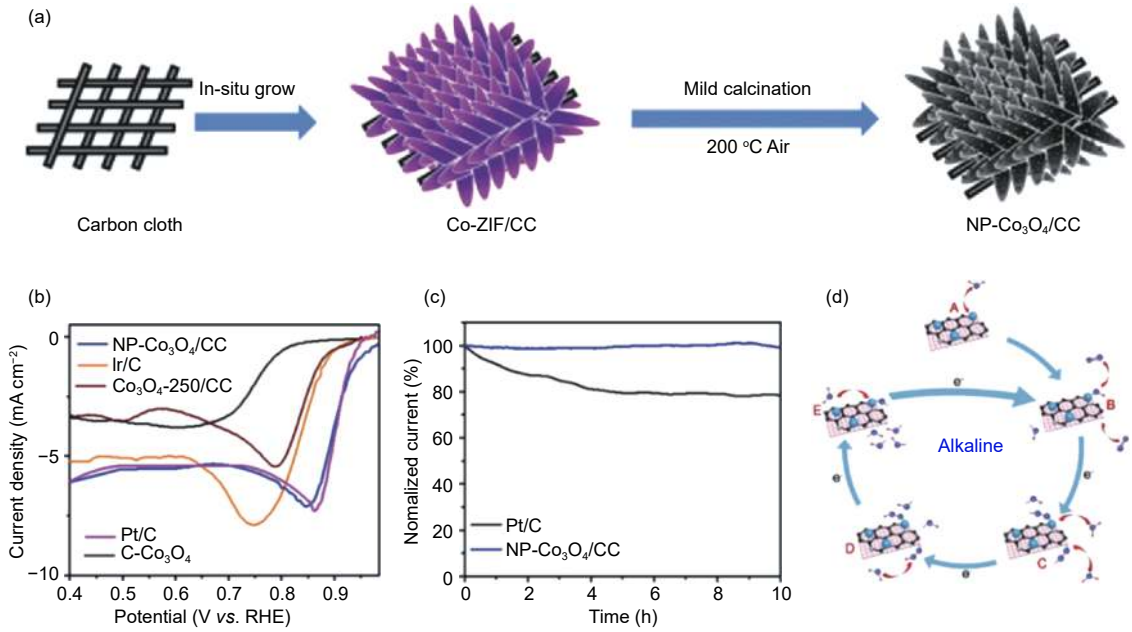

Fig. 4 (a) Schematic illustration for the synthesis of NP-Co_3O_4/CC, (b) polarization curves of various catalysts, (c) the ORR stability evaluation of NP-Co_3O_4/CC and Pt/C (Reprinted with permission by copyright 2020, Elsevier[76]) and (d) schematic illustration of possible ORR mechanisms using Co_3O_4@NGC@MP-TiO_2 catalyst (Reprinted with permission by copyright 2021, Elsevier[77]).

CuO can protect the Co_3O_4 from avoiding undesirable oxidation. The Co_3O_4@NGC@CuO has a $E_{1/2}$ of 0.865 V, comparable to that of commercial Pt/C.

7 Carbon-supported M-S_x-based catalysts for ORR

As a viable catalyst for ORR, iron series metal sulfides are expected to be used as an effective substitute for Pt-based electrocatalysts. The metal cation *d* orbital electron layer in transition metal sulfides is easy to gain or lose electrons, so it is often used in electrochemical catalysis[79]. Theoretical calculation shows that the electrocatalytic ORR performance of cobalt sulfide is similar to that of Pt. However, the catalytic activity of pure cobalt sulfide with different polyvalence states is still much lower than expected[80]. In order to expose more active sites, nanostructured cobalt sulfide is usually loaded on carbon frameworks, which can be beneficial for achieving shortened ion and electron transport distance, and fast reaction kinetics.

Cobalt sulfides with different stoichiometric ratios have been previously explored as excellent electrocatalysts. However, the easy agglomeration and low electrical conductivity of cobalt sulfides result in the unsatisfactory ORR activities. Due to the different of Fermi energy levels between carbon and cobalt sulfides, charge transfer usually occurs at the interface of carbon and cobalt sulfides[83]. Therefore, many researchers have reported that cobalt sulfides coupled with carbon materials exhibit excellent ORR activities. Qiao et al. synthesized $Co_{1-x}S$/N–S–G by embedding cobalt sulfide hollow nanospheres in N and S co-doped graphene[84]. The $Co_{1-x}S$/N–S–G exhibits outstanding ORR catalytic performance with an E_{onset} of 0.978 V and a $E_{1/2}$ of 0.862 V. The excellent electrocatalytic performance of $Co_{1-x}S$/N–S–G is ascribed to the strong interaction between cobalt sulfide hollow nanospheres and graphene. As shown in Fig. 5a, He et al. synthesized a core-shell structure with cobalt sulfide nanowires as the core and N, S codoped graphitic carbon as the shell (CoS NWs@NSC)[81]. The excellent ORR catalytic activity of CoS NWs@NSC can be attributed to the synergistic effect of large surface area, three-dimensional network and abundant accessible active sites. Yao et al. found that the ORR catalytic performance of an octahedral CoS_2 was better than that of a flower-like CoS[85]. There is a high electron density around S—S bond of S_2^{2-}, which can boost the absorption of oxygen on the catalyst surface and facil-

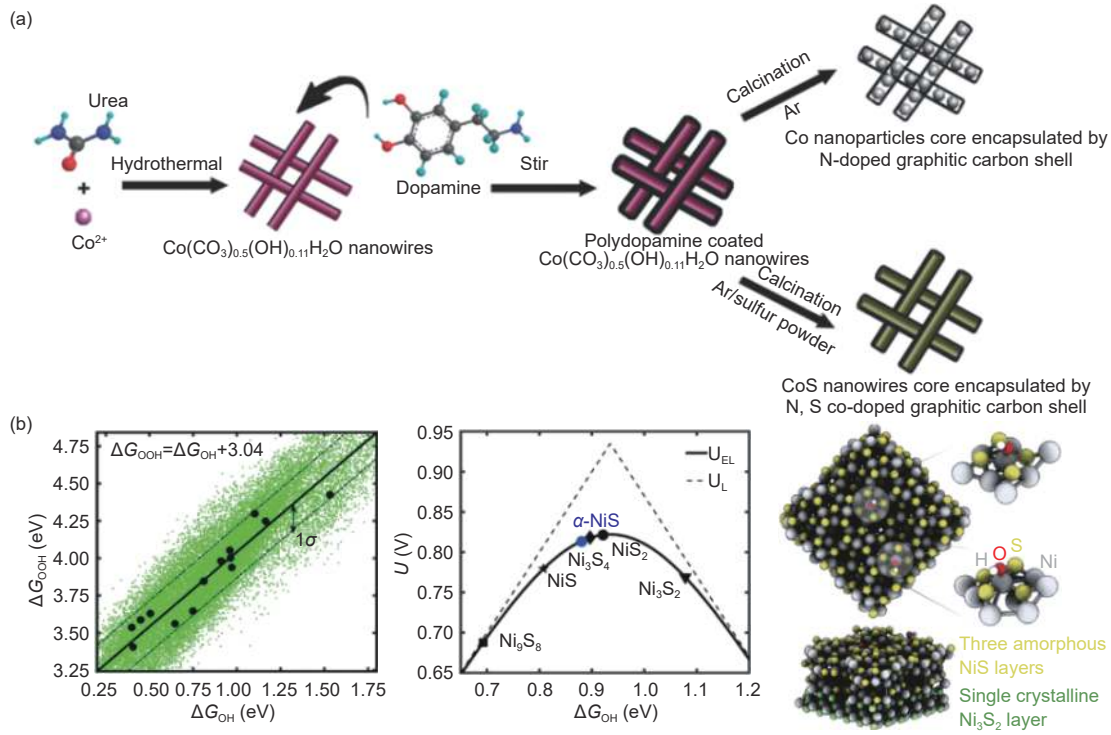

Fig. 5　(a) Schematic illustration for the synthesis of CoS NWs@NSC (Reprinted with permission by copyright 2018, Willey[81]) and (b) ORR activity predictions of NiS_x based on DFT calculations (Reprinted with permission by copyright 2017, Elsevier[82]).

itate the break of the O—O bond in oxygen, resulting in direct $4e^-$ transfer ORR.

One of the notable advantages of nickel sulfide is the higher conductivity than its oxide counterpart, which is important for the electrocatalytic activity. Nickel sulfide has the characteristics of fast charge transfer, strong chemical corrosion resistance, and rich valence state. Sulfur ions in sulfur-rich phase NiS_x have high electron density, which is beneficial for supplying electrons in ORR. Sumboja et al. synthesized a composite of sulfur-rich colloidal nickel sulfides and sulfur-doped reduced graphene oxide (NiS_x/S-rGO)[86]. The S-rGO support with high electrical conductivity enhances the electron transport, and promotes the uniform dispersion of NiS_x during the synthesis process. The NiS_x/S-rGO demonstrates a high E_{onset} of 0.91 V, suggesting the excellent ORR catalytic activity. The excellent ORR catalytic activity of Ni_3S_2 has also been verified. Yan et al. synthesized amorphous carbon layer coated Ni_3S_2 nanoparticles (Ni-NSPC) through directly carbonizing a Ni based MOF[87]. In order to determine the effect of Ni_3S_2, Ni-NSPC was treated with different concentrations of HCl aqueous solutions for controlling the amount of Ni_3S_2, which can be found that an appropriate amount of Ni_3S_2 is very important for ORR. Yan et al. prepared pure Ni_3S_2 by pyrolysis of the mixture of Ni powder and sulfur powder for ORR[82]. However, it is found that the NiS transformed from Ni_2S_3 is the real catalytic site during the electrochemical measurement. As shown in Fig. 5b, DFT calculations show that the Ni-S coordination number of the exposed sites on the surface of nickel sulfide can determine the catalytic activity. Coincidentally, the carbonization of S/Ni(II)-containing polypyrrole solid precursors produced a core-shell structure with Ni_3S_2 core and N, S, O codoped graphitic carbon shell (Ni_3S_2/NOSCs), and the Ni_3S_2/NOSCs was treated with HCl to form NiS shell[21]. The nanoparticles with Ni_3S_2 as the core and NiS as the shell coated with a N-, O- and S-doped carbon (Ni_3S_2/NiS/NOSCs) have excellent electrocatalytic performance toward ORR, which is ascribed to the outstanding conductivity enabled by the carbon layer, the synergistic catalytic effect of inner nickel sulfides and carbon shells, and the electron transfer between Ni_3S_2 and NiS in the Ni_3S_2/NiS core-shell architecture.

8 Carbon-supported iron series metal nanoparticles-based catalysts for ORR

Iron series metal nanoparticles have attracted increasing attention owing to their excellent structural properties[24]. However, the agglomeration and large size of iron series metal nanoparticles may seriously affect the oxygen reduction activity. By reducing the size of the nanoparticles to the level of single atoms or clusters, high catalytic ORR performance can be achieved[88]. Moreover, the coating of carbon layers on the outside of transition metals can be more tolerant to alkaline reaction environments, leading to more stable ORR performance.

Zero-valent cobalt is often neglected in ORR catalysis[90]. The results demonstrate that even if there is no nitrogen doping in the carbon, the zero-valent cobalt can efficiently enhance the ORR activity of the adjacent carbon. Therefore, Co nanoparticles is considered as a kind of hopeful non-noble metal catalyst owing to the characters of low cost, high catalytic activity, simple preparation, and long-term operation stability. Rao et al. prepared a core-shell structured catalyst with the Co core and N doped carbon nanotube shell (Co@NCNT-300-5) by programmed carbonization with additional plasma etching[91]. The E_{onset} and $E_{1/2}$ of the Co@NCNT-300-5 are 1.030 V and 0.872 V, respectively, which are superior to those of Pt/C. Such outstanding ORR catalytic performance of Co@NCNT-300-5 can be attributed to the unique core-shell nanostructures and more microcracks on the carbon shell caused by plasma corrosion for providing rich accessible defects and active sites. As shown in Fig. 6a, Liu et al. introduced Co nanoparticles into S and N co-doped carbon nanotubes (Co@SNHC) by pyrolyzing the mixture of sublimed sulfur, melamine, cobalt acetate and SiO_2@resorcinol–formaldehyde spheres[89]. The Co@SNHC exhibits excellent ORR performance with a high $E_{1/2}$ of 0.831 V under alkaline conditions. The outstanding ORR performance of Co@SNHC is due to the following reasons. (i) The coating of carbon layers causes the decreased local work function of cobalt nanoparticles. (ii) The introduction of heteroatoms leads to the generation of carbon atoms with uneven charge, which is beneficial for adsorbing oxygen species. Similarly, high performance ORR catalysts can be achieved by encapsulating Ni nanoparticles in N-doped porous carbon nanocapsules to form a nanoreactor[22]. As shown in Fig. 6b-6c, the $E_{1/2}$ and stability of the encapsulating Ni nanoparticles in the N-doped porous carbon is superior to those loaded on the outer surface of a N-doped porous carbon. According to the experimental and DFT analysis, the existence of Ni nanoparticles can immensely enhance ORR catalytic activity. After O_2 molecules pass through the graphitic carbon layer, the oxygen can be confined in a limited space, leading to the increased contact probability between active sites and O_2. This result indicates that the formed nanoreactor can increase the reaction rate for reducing O_2, which ultimately improves the catalytic activity.

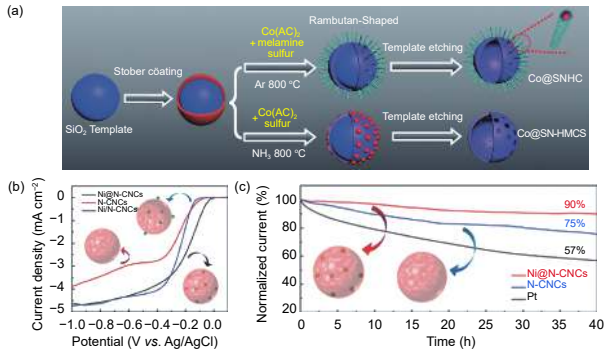

Fig. 6 (a) Schematic illustration of the preparation of Co@SNHC (Reprinted with permission by copyright 2019, RSC[89]) , (b) rotating disk electrode (RDE) polarization curves of Ni@N-CNCs, N-CNCs, and Ni/N-CNCs and (c) chronoamperometric response of Pt/C, Ni@N-CNCs, and N-CNCs at −0.4 V and 1 600 r/min (Reprinted with permission by copyright 2017, Willey[22]).

9 Carbon-supported Fe-C_x-based catalysts for ORR

During the calcination process, iron can easily react with carbon to form the iron carbide, and iron carbide encapsulated in graphitic carbon layers is known as excellent ORR catalytic active center[94]. As shown in Fig. 7a, the core-shell structured catalyst was generated through the incorporation of Fe_3C into carbon materials[92]. The carbon layer not only pro-

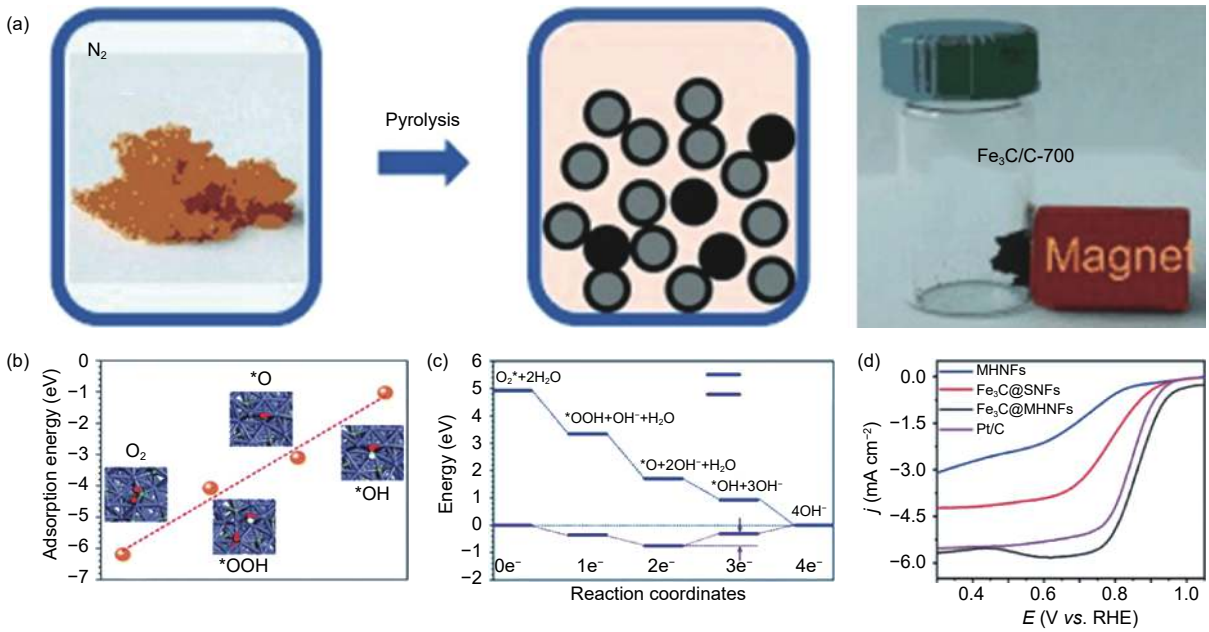

Fig. 7　(a) Schematic illustration of the preparation of Fe_3C/C-700 (Reprinted with permission by copyright 2014, Willy[92]), (b) the linear correlation of adsorption energies for intermediates during ORR, (c) the energetic pathway of the ORR on Fe_3C@MHNFs and (d) polarization curves of MHNFs, Fe_3C@SNFs, Fe_3C@MHNFs and commercial Pt/C (Reprinted with permission by copyright 2020, RSC[93]).

motes the dispersion of iron carbide nanoparticles, but also prevents the corrosion of iron carbide in the electrolyte. The coating of a graphitic carbon layer on iron carbide nanoparticles can induce unique host-guest electron interactions, and the charge transfer from Fe_3C nanoparticles to carbon reduces the local work function of the carbon layer, thus promoting the adsorption and reduction of O_2, which is of great significance for improving the catalytic activity of ORR. Xia et al. reported the confinement of Fe_3C nanoparticles into multichannel hollow carbon nanofibers (Fe_3C@MHNFs) by using electrospinning technique[93]. The $E_{1/2}$ of Fe_3C@MHNFs is 0.90 V, which is better than that of Pt/C (0.81 V). The novel hollow structured carbon matrix and the high activity Fe_3C nanoparticles enhance the catalytic activity of hybrid products for ORR. As shown in Fig. 7b and 7c, DFT calculations show that the electron transfer efficiency of the catalyst is greatly improved because of the generation of a highly electroactive interface region for optimizing the electronic environment, and promotes the binding and conversion of intermediates. As a result, Fe_3C@MHNFs shows excellent ORR performance with a $E_{1/2}$ of 0.831 V (Fig. 7d).

10　Multiple active sites for ORR

Generally, the catalyst with multi-components can provide a variety of catalytic active species, and the synergistic effect generated among the components can play a positive role in promoting the ORR performance. Rich interfaces can be formed by the heterogeneous structure in catalysts. At the same time, the electron aggregation occurs at the interface of different substances, and the conductive electrons can be easily transferred at interfaces, which can produce unexpected ORR activity. Therefore, the design of catalysts with multiple transition metal species is promising for improving the electrocatalytic ORR activity.

The catalytic activity of FeO_x is very low, but the combination of FeO_x with other active sites can produce largely enhanced catalytic activity. Xiao et al. proposed a H_2-thermal-reduction strategy to prepare FeO_x/Fe heterostructures embedded in a N-doped porous carbon framework (Fe_2O_3@NC-450) (Fig. 8a)[95]. The H_2 treatment temperature can effectively affect ORR performance. When the treatment temperature is 450 °C, the formed FeO_x/Fe heterostructure, the multiple exposed crystal faces, and interaction between FeO_x/Fe and the nitrogen doped carbon layer result in

the high conductivity, good hydrophilicity, and good stability of Fe_2O_3@NC-450, which can greatly improve the ORR performance. Lei et al. prepared Fe single atom sites and ultra-small Fe_2O_3 nanoclusters embedded in a N, S co-doped porous carbon as effective ORR catalysts (Fe_{SA}/FeO_{NC}/NSC) (Fig. 8b-c)[96]. The outstanding ORR behavior of Fe_{SA}/FeO_{NC}/NSC is ascribed to the following reasons. (i) Fe single atomic sites integrated with Fe_2O_3 clusters act as highly active sites. (ii) The doping of N and S can lead to the uneven charge distribution in the carbon matrix for facilitating the adsorption of oxygen. (iii) Porous carbon frameworks with ultra-thin edges make active species more accessible for ORR reaction.

Tan et al. synthesized Co-CoO multiphase nanoparticles coated with N, S co-doped carbon shells (Co-CoO@NSC) by pyrolyzing ZIF-67 with thiourea for *in situ* S doping[98]. The Co-CoO@NSC exhibits excellent catalytic activity with an $E_{1/2}$ of 0.89 V. The carbon layer serves as electron channels for the encapsulated Co-CoO nanoparticles, and DFT calculations show that S doping reduces the formation energy of OOH* on Co-N_4 sites and Co-O-C. Hu et al. synthesized the Co nanoparticle-embedded in double-shelled carbon@Co_9S_8 nanocages (Co-C@Co_9S_8 DSNCs) by a MOF-engaged strategy[99]. The inner Co nanoparticles embedded in the carbon are catalytic centers in Co-C@Co_9S_8 DSNCs, while the outer carbon and Co_9S_8 shells not only allow reactants to the active sites, but also prevent the Co nanoparticles from aggregation and leaching out. The Co-C@Co_9S_8 DSNCs acts as nanoreactors for providing high driving force for the ORR. Tian et al. synthesized a nanocomposite with heterogenous CoS/CoO nanocrystals loaded on N-doped graphene (CoS/CoO@NGNs)[100]. The CoS/CoO@NGNs shows an excellent ORR activity with an $E_{1/2}$ of 0.84 V, equal to that of Pt/C. The CoS/CoO interface structure with the coupling effect between

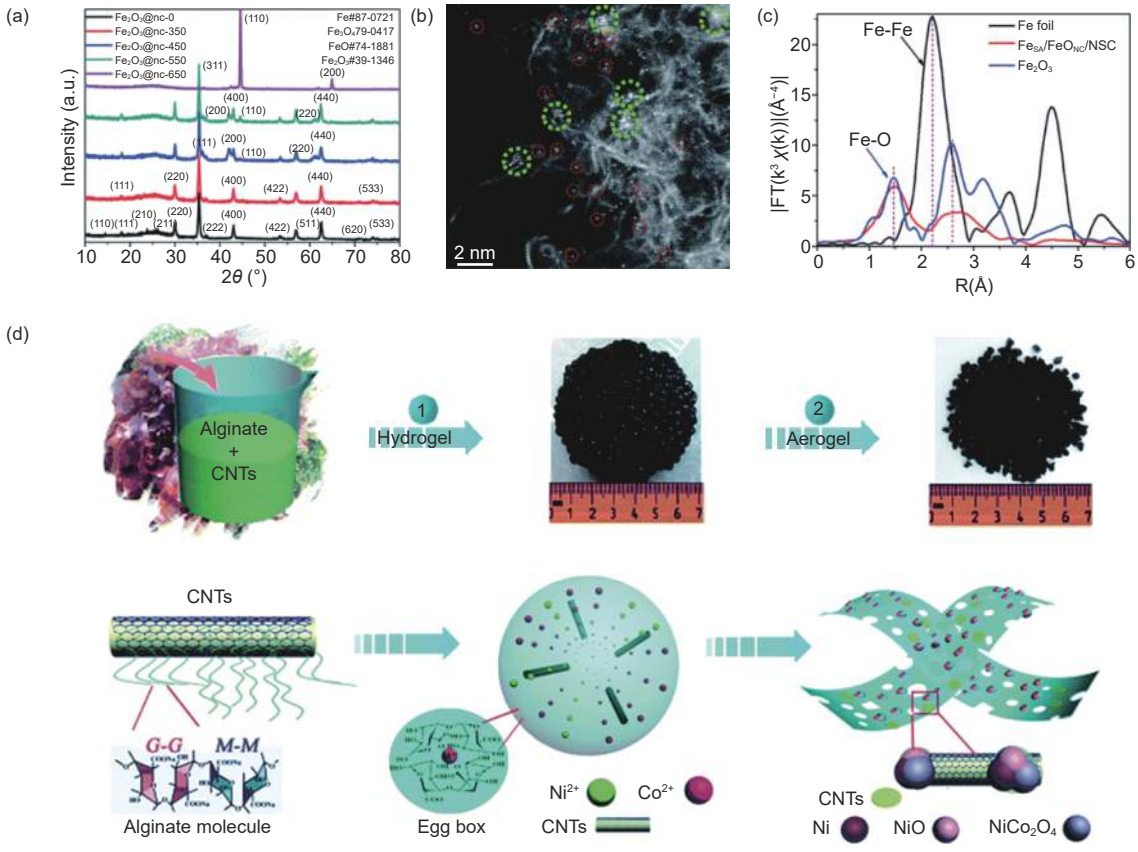

Fig. 8 (a) XRD patterns of the Fe_2O_3@NC-450 (Reprinted with permission by copyright 2020, RSC[95]), (b) high-angle annular dark field-scanning transmission election microscope (HAADF-STEM) images of Fe_{SA}/FeO_{NC}/NSC, (c) Fe K-edge k^3-weighted Fourier transform (FT) spectra of Fe_{SA}/FeO_{NC}/NSC, Fe_2O_3 and Fe foil (Reprinted with permission by copyright 2020, RSC[96]) and (d) schematic illustration of the preparation of Ni/NiO/$NiCo_2O_4$/N-CNT-As (Reprinted with permission by copyright 2016, RSC[97]).

CoS/CoO and N-doped graphene can improve the conductivity, accelerate the electron transfer, and improve the stability of the catalyst. Peng et al. prepared Co nanoparticles anchored in N-doped hollow porous carbon nanofibers (CoN-HPCNF) by an in-situ growth pyrolysis method using ZIF-67 as a precursor[101]. The excellent ORR property of CoN-HPCNF is attributed to the high specific surface area, abundant hierarchical porous structure, and ample active sites from the graphic N, pyridinic N, Co-N, and Co particles.

As shown in Fig. 8d, Ma et al. synthesized a N doped carbon nanotube aerogel loaded with Ni/NiO/$NiCo_2O_4$ nanoparticles by using an alginate derived biomass conversion strategy (Ni/NiO/$NiCo_2O_4$/N-CNT-As)[97]. The excellent ORR catalytic activity of Ni/NiO/$NiCo_2O_4$/N-CNT-As can be attributed to the following reasons. (i) NiO and $NiCo_2O_4$ have strong affinity for O atoms in OH^-, which weakens the binding force of O–H bond. (ii) Ni has affinity for H atom, which can help dissociate H and promote the fracture of O–H bond. (iii) The carbon nanotube aerogel carrier has rich pore structure and good conductivity, which greatly enhances the kinetics and catalytic activity.

Reasonable combination of multiple active sites can not only improve the catalytic activity, but also realize the preparation of multifunctional catalysts. Our group used NaH_2PO_2 as the template, iron chelated sodium lignosulfonate as the precursor and ammonia as the nitrogen source to couple Fe-N-C and FeP into N, P and S co-doped carbon skeleton (Fe-N-C/FeP_x/NPSC) for realizing trifunctional catalysis[102]. The Fe-N-C/FeP_x/NPSC displays outstanding catalytic performances for ORR, OER and HER. The excellent multifunctional electrocatalytic properties of Fe-N-C/FeP_x/NPSC can be attributed to the following reasons. (i) The coupling of multiple active sites not only maintains the intrinsic activity of each site, but also improves the catalytic activity through a synergistic effect. (ii) Large specific surface area and developed pore structure can expose more active sites and promote mass/electron transfer. (iii) The carbon support can effectively promote the dispersity of active sites for improving the stability of the catalyst.

11　Summary and perspective

In general, the iron series catalysts have shown fascinating activity in ORR, owing to their low cost and high efficiency. In this review, we have summarized several iron series catalysts and analyzed the possible mechanisms and influencing factors towards ORR. We discuss the change of electron and structure composition in iron series catalysts, and clarify the intrinsic character for affecting the catalytic reactions. The catalytic activity of ORR can be improved by coupling nonmetallic heteroatoms and iron series elements into the carbon framework, and controlling the morphology and size of the iron series element-based compounds. Importantly, the introduction of carbon materials can be beneficial for obtaining well-dispersed active sites and largely exposed surface area, leading to shortened transport pathway of ions/electrons and accelerated reaction kinetics.

It is undoubted that the introduction of iron series elements is very important to improve the ORR activity of materials. However, the development of the more efficient iron series element based catalysts still remains a huge challenge in the future. Firstly, the specific role of each iron series elements in the catalysts has not been well-understood. The researchers usually claim that there are synergistic effects among multiple active sites, and it is really necessary to clarify the activity origins and realize the identification of active sites. The determination of the catalytic mechanisms for each active site is beneficial for developing new-type catalysts. In recent years, the catalysis mechanism of M-N_x has been studied extensively, but the catalysis mechanism of other iron series compounds needs to be further explored. Secondly, the performance of active sites is considered to be closely related with their morphology and size, and the porous structure and microstructure of the catalysts. Therefore, it is necessary and important to design iron series element based catalysts with finely tuned structures (such as defects, porosity, interfaces and surfaces). Thirdly, the interaction of multiple active sites

plays a vital role in improving the catalytic ability. Combining different active sites through interfacial engineering is a promising strategy, which can not only lead to the enhancement of ORR performance, but also realize the construction of bi/trifunctional catalysts (ORR/OER and ORR/OER/HER) at the same time. Overall, the opportunities and challenges are coexisted for ORR catalysts, and we believe that iron series catalysts can be close to practical applications in the near future, especially matching the current worldwide demand on noble metal free catalysts.

Acknowledgements

Shandong Provincial Natural Science Foundation, China (No.ZR2020ME038); Shandong Provincial Key R&D Plan and the Public Welfare Special Program, China (No.2019GGX102038); Fundamental Research Funds for the Central Universities (No. 201941010 and 201822008); Qingdao City Programs for Science and Technology Plan Projects (19-6-2-77-cg); National Natural Science Foundation of China (No.21471139).

References

[1] Zhou M, Wang H, Guo S. Towards high-efficiency nanoelectrocatalysts for oxygen reduction through engineering advanced carbon nanomaterials[J]. Chemical Society Reviews, 2016, 45(5): 1273-1307.

[2] Li J, Hou P, Liu C. Heteroatom-doped carbon nanotube and graphene-based electrocatalysts for oxygen reduction reaction[J]. Small, 2017, 13(45): 1702002.

[3] Zhang J, Zhang J, He F, et al. Defect and doping Co-engineered non-metal nanocarbon ORR electrocatalyst[J]. Nano-Micro Letters, 2021, 13(1): 65.

[4] Yang L, Shui J, Lei D, et al. Carbon-based metal-free ORR electrocatalysts for fuel cells: Past, present, and future[J]. Advanced Materials, 2019, 31(13): 1804799.

[5] Mamtani K, Jain D, Dogu D, et al. Insights into oxygen reduction reaction (ORR) and oxygen evolution reaction (OER) active sites for nitrogen-doped carbon nanostructures (CN_x) in acidic media[J]. Applied Catalysis B: Environmental, 2018(220): 88-97.

[6] Ding D, Shen K, Chen X, et al. Multi-level architecture optimization of MOF-templated Co-based nanoparticles embedded in hollow N-doped carbon polyhedra for efficient OER and ORR[J]. ACS Catalysis, 2018, 8(9): 7879-7888.

[7] Blaser H U. Catalysis without Precious Metals[M]. Edited by R Morris Bullock[J]. ChemCatChem, 2011, 3(4): 780-780.

[8] Chirik P J. Carbon–carbon bond formation in a weak ligand field: Leveraging open-shell first-row transition-metal catalysts[J]. Angewandte Chemie International Edition, 2017, 56(19): 5170-5181.

[9] Schröder D, Shaik S, Schwarz H. Two-state reactivity as a new concept in organometallic chemistry[J]. Accounts of Chemical Research, 2000, 33(3): 139-145.

[10] Jin J, Yin J, Liu H, et al. Transition metal (Fe, Co and Ni)−carbide−nitride (M−C−N) nanocatalysts: Structure and electrocatalytic applications[J]. ChemCatChem, 2019, 11(12): 2780-2792.

[11] Wang Y, Li J, Wei Z. Transition-metal-oxide-based catalysts for the oxygen reduction reaction[J]. Journal of Materials Chemistry A, 2018, 6(18): 8194-8209.

[12] Liang Z, Zheng H, Cao R. Recent advances in Co-based electrocatalysts for the oxygen reduction reaction[J]. Sustainable Energy & Fuels, 2020, 4(8): 3848-3870.

[13] Xu Z, Zhao H, Liang J, et al. Noble-metal-free electrospun nanomaterials as electrocatalysts for oxygen reduction reaction[J]. Materials Today Physics, 2020(15): 100280.

[14] Li Y, Chen B, Duan X, et al. Atomically dispersed Fe-N-P-C complex electrocatalysts for superior oxygen reduction[J]. Applied Catalysis B: Environmental, 2019(249): 306-315.

[15] Li W, Chen J, Xiao Z, et al. MoS_2/graphene/carbonized melamine foam composite catalysts for the hydrogen evolution reaction[J]. New Carbon Materials, 2020, 35(5): 540-546.

[16] Gong X, Zhu J, Li J, et al. Self-templated hierarchically porous carbon nanorods embedded with atomic Fe-N_4 active sites as efficient oxygen reduction electrocatalysts in Zn-air batteries[J]. Advanced Functional Materials, 2021, 31(8): 2008085.

[17] Chen J, Li H, Fan C, et al. Dual single-atomic Ni-N_4 and Fe-N_4 sites constructing janus hollow graphene for selective oxygen electrocatalysis[J]. Advanced Materials, 2020: e2003134.

[18] Wang B, Ye Y, Xu L, et al. Space-confined yolk-shell construction of Fe_3O_4 nanoparticles inside N-doped hollow mesoporous carbon spheres as bifunctional electrocatalysts for long-term rechargeable zinc –air batteries[J]. Advanced Functional Materials, 2020, 30(51): 2005834.

[19] Singh K P, Bae E J, Yu J S. Fe-P: A new class of electroactive catalyst for oxygen reduction reaction[J]. Journal of the American Chemical Society, 2015, 137(9): 3165-3168.

[20] Cai Z, Du P, Liang W, et al. Single-atom-sized Ni –N_4 sites anchored in three-dimensional hierarchical carbon nanostructures for the oxygen reduction reaction[J]. Journal of Materials Chemistry A, 2020, 8(30): 15012-15022.

[21] Cao Y, Meng Y, Huang S, et al. Nitrogen-, oxygen- and sulfur-doped carbon-encapsulated Ni_3S_2 and NiS core–shell architectures: bifunctional electrocatalysts for hydrogen evolution and oxygen reduction reactions[J]. ACS Sustainable Chemistry & Engineering, 2018, 6(11): 15582-15590.

[22] Li B, Nam H, Zhao J, et al. Nanoreactor of nickel-containing carbon –shells as oxygen reduction catalyst[J]. Advanced

Materials, 2017, 29(7): 1605083.

[23] Liu P, Ran J, Xia B, et al. Bifunctional oxygen electrocatalyst of mesoporous Ni/NiO nanosheets for flexible rechargeable Zn–air batteries[J]. Nano-Micro Letters, 2020, 12(1): 68.

[24] Liu T, Mou J, Wu Z, et al. A facile and scalable strategy for fabrication of superior bifunctional freestanding air electrodes for flexible zinc–air batteries[J]. Advanced Functional Materials, 2020, 30(36): 2003407.

[25] Guo X, Zhang W, Zhang D, et al. Submicron Co_9S_8/CoS/carbon spheres derived from bacteria for the electrocatalytic oxygen reduction reaction[J]. ChemElectroChem, 2019, 6(17): 4571-4575.

[26] Zhang Y, Tao H, Chen Z, et al. In situ grown cobalt phosphide (CoP) on perovskite nanofibers as an optimized trifunctional electrocatalyst for Zn–air batteries and overall water splitting[J]. Journal of Materials Chemistry A, 2019, 7(46): 26607-26617.

[27] Yang Q, Jia Y, Wei F, et al. Understanding the activity of Co-$N_{4-x}C_x$ in atomic metal catalysts for oxygen reduction catalysis[J]. Angewandte Chemie International Edition, 2020, 59(15): 6122-6127.

[28] Wu M, Xie J, Liu A, et al. Iron carbide/nitrogen-doped carbon core-shell nanostrctures: Solution-free synthesis and superior oxygen reduction performance[J]. Journal of Colloid and Interface Science, 2020(566): 194-201.

[29] Borghei M, Lehtonen J, Liu L, et al. Advanced biomass-derived electrocatalysts for the oxygen reduction reaction[J]. Advanced Materials, 2018, 30(24): 1870171.

[30] Fukuzumi S, Lee Y-M, Nam W. Mechanisms of two-electron versus four-electron reduction of dioxygen catalyzed by earth-abundant metal complexes[J]. ChemCatChem, 2018, 10(1): 9-28.

[31] Ouyang D, Hu L, Wang G, et al. A review of biomass-derived graphene and graphene-like carbons for electrochemical energy storage and conversion[J]. New Carbon Materials, 2021, 36(2): 350-372.

[32] Singh S K, Takeyasu K, Nakamura J. Active sites and mechanism of oxygen reduction reaction electrocatalysis on nitrogen-doped carbon materials[J]. Advanced Materials, 2019, 31(13): e1804297.

[33] Ye X, Hu L, Liu M, et al. Improved oxygen reduction performance of a N, S co-doped graphene-like carbon prepared by a simple carbon bath method[J]. New Carbon Materials, 2020, 35(5): 531-539.

[34] Ding Y, Kopold P, Hahn K, et al. Facile solid-state growth of 3D well-interconnected nitrogen-rich carbon nanotube–graphene hybrid architectures for lithium–sulfur batteries[J]. Advanced Functional Materials, 2016, 26(7): 1112-1119.

[35] Chen Y, Wang J, Liu H, et al. Nitrogen doping effects on carbon nanotubes and the origin of the enhanced electrocatalytic activity of supported Pt for proton-exchange membrane fuel cells[J]. The Journal of Physical Chemistry C, 2011, 115(9): 3769-3776.

[36] Wei P, Yu G, Naruta Y, et al. Covalent grafting of carbon nanotubes with a biomimetic heme model compound to enhance oxygen reduction reactions[J]. Angewandte Chemie International Edition, 2014, 53(26): 6659-6663.

[37] Shi J, Lin N, Lin H, et al. A N-doped rice husk-based porous carbon as an electrocatalyst for the oxygen reduction reaction[J]. New Carbon Materials, 2020, 35(4): 401-409.

[38] Chen P, Xiao T, Qian Y, et al. A nitrogen-doped graphene/carbon nanotube nanocomposite with synergistically enhanced electrochemical activity[J]. Advanced Materials, 2013, 25(23): 3192-3196.

[39] Yang Z, Yang Y, Lu C, et al. A high energy density fiber-shaped supercapacitor based on zinc-cobalt bimetallic oxide nanowire forests on carbon nanotube fibers[J]. New Carbon Materials, 2019, 34(6): 559-568.

[40] Luo E, Chu Y, Liu J, et al. Pyrolyzed M–N_x catalysts for oxygen reduction reaction: progress and prospects[J]. Energy & Environmental Science, 2021, 14(4): 2158-2185.

[41] Du Z, Shen S, Tang Z, et al. Graphene quantum dots-based heterogeneous catalysts[J]. New Carbon Materials, 2021, 36(3): 449-467.

[42] Yan X, Jia Y, Wang K, et al. Controllable synthesis of Fe–N_4 species for acidic oxygen reduction[J]. Carbon Energy, 2020, 2(3): 452-460.

[43] Liu K, Wu G, Wang G. Role of local carbon structure surrounding FeN_4 sites in boosting the catalytic activity for oxygen reduction[J]. The Journal of Physical Chemistry C, 2017, 121(21): 11319-11324.

[44] Zitolo A, Goellner V, Armel V, et al. Identification of catalytic sites for oxygen reduction in iron- and nitrogen-doped graphene materials[J]. Nature Materials, 2015, 14(9): 937-942.

[45] He Y, Liu S, Priest C, et al. Atomically dispersed metal–nitrogen–carbon catalysts for fuel cells: Advances in catalyst design, electrode performance, and durability improvement[J]. Chemical Society Reviews, 2020, 49(11): 3484-3524.

[46] Li J, Zhang H, Samarakoon W, et al. Thermally driven structure and performance evolution of atomically dispersed FeN_4 sites for oxygen reduction[J]. Angewandte Chemie International Edition, 2019, 58(52): 18971-18980.

[47] Shao C, Zhuang S, Zhang H, et al. Enhancement of mass transport for oxygen reduction reaction using petal-like porous Fe-NC nanosheet[J]. Small, 2021, 17(6): 2006178.

[48] Huo J, Lu L, Shen Z, et al. A rational synthesis of single-atom iron–nitrogen electrocatalysts for highly efficient oxygen reduction reaction[J]. Journal of Materials Chemistry A, 2020, 8(32): 16271-16282.

[49] Ge H, Li G, Shen J, et al. Co_4N nanoparticles encapsulated in N-doped carbon box as tri-functional catalyst for Zn-air battery and overall water splitting[J]. Applied Catalysis B: Environmental, 2020(275): 119104.

[50] Kattel S, Atanassov P, Kiefer B. Density functional theory study of Ni–N_x/C electrocatalyst for oxygen reduction in alkaline and acidic media[J]. The Journal of Physical Chemistry C, 2012,

116(33): 17378-17383.

[51] Liang Z, Luo M, Chen M, et al. Exploring the oxygen electrode bi-functional activity of Ni–N–C-doped graphene systems with N, C co-ordination and OH ligand effects[J]. Journal of Materials Chemistry A, 2020, 8(39): 20453-20462.

[52] Jasinski R. A new fuel cell cathode catalyst[J]. Nature, 1964, 201(4925): 1212-1213.

[53] Zhang J, Song L, Zhao C, et al. Co, N co-doped porous carbons as high-performance oxygen reduction electrocatalysts[J]. New Carbon Materials, 2021, 36(1): 209-218.

[54] Shu X, Chen S, Chen S, et al. Cobalt nitride embedded holey N-doped graphene as advanced bifunctional electrocatalysts for Zn-Air batteries and overall water splitting[J]. Carbon, 2020(157): 234-243.

[55] Sun X, Sun S, Gu S, et al. High-performance single atom bifunctional oxygen catalysts derived from ZIF-67 superstructures[J]. Nano Energy, 2019(61): 245-250.

[56] Cai Z, Lin S, Xiao J, et al. Efficient bifunctional catalytic electrodes with uniformly distributed NiN_2 active sites and channels for long-lasting rechargeable zinc –air batteries[J]. Small, 2020, 16(32): 2002518.

[57] Yang D S, Bhattacharjya D, Inamdar S, et al. Phosphorus-doped ordered mesoporous carbons with different lengths as efficient metal-free electrocatalysts for oxygen reduction reaction in alkaline media[J]. Journal of the American Chemical Society, 2012, 134(39): 16127-16130.

[58] Zhang Z, Lv R, Huang Z, et al. Carbon materials for use in the electrocatalytic hydrogen evolution reaction[J]. New Carbon Materials, 2019, 34(2): 115 − 131.

[59] Zhou Y, Xing Y F, Wen J, et al. Axial ligands tailoring the ORR activity of cobalt porphyrin[J]. Science Bulletin, 2019, 64(16): 1158-1166.

[60] Chen L, Zhang Y, Dong L, et al. Honeycomb-like 3D N-, P-codoped porous carbon anchored with ultrasmall Fe_2P nanocrystals for efficient Zn-air battery[J]. Carbon, 2020(158): 885-892.

[61] Liu H, Guan J, Yang S, et al. Metal–organic-framework-derived Co_2P nanoparticle/multi-doped porous carbon as a trifunctional electrocatalyst[J]. Advanced Materials, 2020, 32(36): 2003649.

[62] Li H, Li Q, Wen P, et al. Colloidal cobalt phosphide nanocrystals as trifunctional electrocatalysts for overall water splitting powered by a zinc –air battery[J]. Advanced Materials, 2018, 30(9): 1705796.

[63] He F, Li K, Xie G, et al. Theoretical insights on the catalytic activity and mechanism for oxygen reduction reaction at Fe and P codoped graphene[J]. Physical Chemistry Chemical Physics, 2016, 18(18): 12675-12681.

[64] Feng L, Liu Y, Zhao J. Fe– and Co–P_4-embedded graphenes as electrocatalysts for the oxygen reduction reaction: theoretical insights[J]. Physical Chemistry Chemical Physics, 2015, 17(45): 30687-30694.

[65] Yang W, Liu X, Lv H, et al. Atomic Fe & FeP nanoparticles synergistically facilitate oxygen reduction reaction of hollow carbon hybrids[J]. Journal of Colloid and Interface Science, 2021(583): 371-375.

[66] Li M, Liu T, Bo X, et al. Hybrid carbon nanowire networks with Fe –P bond active site for efficient oxygen/hydrogen-based electrocatalysis[J]. Nano Energy, 2017(33): 221-228.

[67] Liao H, Sun Y, Dai C, et al. An electron deficiency strategy for enhancing hydrogen evolution on CoP nano-electrocatalysts[J]. Nano Energy, 2018(50): 273-280.

[68] Yang F, Chen Y, Cheng G, et al. Ultrathin nitrogen-doped carbon coated with CoP for efficient hydrogen evolution[J]. ACS Catalysis, 2017, 7(6): 3824-3831.

[69] Hao Y, Xu Y, Liu W, et al. Co/CoP embedded in a hairy nitrogen-doped carbon polyhedron as an advanced tri-functional electrocatalyst[J]. Materials Horizons, 2018, 5(1): 108-115.

[70] Cheng Y, Liao F, Shen W, et al. Carbon cloth supported cobalt phosphide as multifunctional catalysts for efficient overall water splitting and zinc–air batteries[J]. Nanoscale, 2017, 9(47): 18977-18982.

[71] Wang Y, Wu M, Li J, et al. In situ growth of CoP nanoparticles anchored on (N, P) co-doped porous carbon engineered by MOFs as advanced bifunctional oxygen catalyst for rechargeable Zn–air battery[J]. Journal of Materials Chemistry A, 2020, 8(36): 19043-19049.

[72] Meng T, Hao Y, Zheng L, et al. Organophosphoric acid-derived CoP quantum dots@S, N-codoped graphite carbon as a trifunctional electrocatalyst for overall water splitting and Zn–air batteries[J]. Nanoscale, 2018, 10(30): 14613-14626.

[73] Li Y, Liu Y, Qian Q, et al. Supramolecular assisted one-pot synthesis of donut-shaped CoP@PNC hybrid nanostructures as multifunctional electrocatalysts for rechargeable Zn-air batteries and self-powered hydrogen production[J]. Energy Storage Materials, 2020(28): 27-36.

[74] Li H, Zhang H, Yan X, et al. Carbon-supported metal single atom catalysts[J]. New Carbon Materials, 2018, 33(1): 1-11.

[75] Wang Y, Yu B, Liu K, et al. Co single-atoms on ultrathin N-doped porous carbon via a biomass complexation strategy for high performance metal –air batteries[J]. Journal of Materials Chemistry A, 2020, 8(4): 2131-2139.

[76] Wang X, Liao Z, Fu Y, et al. Confined growth of porous nitrogen-doped cobalt oxide nanoarrays as bifunctional oxygen electrocatalysts for rechargeable zinc –air batteries[J]. Energy Storage Materials, 2020(26): 157-164.

[77] Yu Y, You S, Du J, et al. Ti^{3+}-self-doped TiO_2 with multiple crystal-phases anchored on acid-pickled ZIF-67-derived Co_3O_4@N-doped graphitized-carbon as a durable catalyst for oxygen reduction in alkaline and acid media[J]. Chemical Engineering Journal, 2021(403): 126441.

[78] Du J, You S, Li X, et al. In situ immobilization of copper oxide thin-layer on zeolitic imidazolate framework-67-derived cobalt oxide@nitrogen-doped carbon with multi-level architecture and versatile active sites for enhancing oxygen evolution/reduction

reactions[J]. Journal of Power Sources, 2020(478): 228707.

[79] Tao Y, Kong Z, Wei Y, et al. Synthesis and electrochemical performance of S/mesoporous carbon microsphere-MoS_2 cathode materials[J]. New Carbon Materials, 2019, 34(4): 349 − 357.

[80] Xu Y, Sumboja A, Zong Y, et al. Bifunctionally active nanosized spinel cobalt nickel sulfides for sustainable secondary zinc–air batteries: Examining the effects of compositional tuning on OER and ORR activity[J]. Catalysis Science & Technology, 2020, 10(7): 2173-2182.

[81] Han C, Li Q, Wang D, et al. Cobalt sulfide nanowires core encapsulated by a N, S codoped graphitic carbon shell for efficient oxygen reduction reaction[J]. Small, 2018, 14(17): 1703642.

[82] Yan B, Krishnamurthy D, Hendon C H, et al. Surface restructuring of nickel sulfide generates optimally coordinated active sites for oxygen reduction catalysis[J]. Joule, 2017, 1(3): 600-612.

[83] Higgins D C, Hassan F M, Seo M H, et al. Shape-controlled octahedral cobalt disulfide nanoparticles supported on nitrogen and sulfur-doped graphene/carbon nanotube composites for oxygen reduction in acidic electrolyte[J]. Journal of Materials Chemistry A, 2015, 3(12): 6340-6350.

[84] Qiao X, Jin J, Fan H, et al. In situ growth of cobalt sulfide hollow nanospheres embedded in nitrogen and sulfur co-doped graphene nanoholes as a highly active electrocatalyst for oxygen reduction and evolution[J]. Journal of Materials Chemistry A, 2017, 5(24): 12354-12360.

[85] Yao S, Huang T, Fang H, et al. Cobalt sulfides as efficient catalyst towards oxygen reduction reactions[J]. Chinese Chemical Letters, 2020, 31(2): 530-534.

[86] Sumboja A, Chen J, Ma Y, et al. Sulfur-rich colloidal nickel sulfides as bifunctional catalyst for all-solid-state, flexible and rechargeable Zn-Air batteries[J]. ChemCatChem, 2019, 11(4): 1205-1213.

[87] Yan W, Cao X, Wang R, et al. S, N co-doped rod-like porous carbon derived from S, N organic ligand assembled Ni-MOF as an efficient electrocatalyst for oxygen reduction reaction[J]. Journal of Solid State Chemistry, 2019(275): 167-173.

[88] Liu P, Hao B, Zhang H, et al. Atomic-scale investigation of carbon-based materials by gentle transmission electron microscopy[J]. New Carbon Materials, 2021, 36(3): 497-511.

[89] Liu J, Xu L, Deng Y, et al. Metallic cobalt nanoparticles embedded in sulfur and nitrogen co-doped rambutan-like nanocarbons for the oxygen reduction reaction under both acidic and alkaline conditions[J]. Journal of Materials Chemistry A, 2019, 7(23): 14291-14301.

[90] Tan M, Xiao Y, Xi W, et al. Cobalt-nanoparticle impregnated nitrogen-doped porous carbon derived from Schiff-base polymer as excellent bifunctional oxygen electrocatalysts for rechargeable zinc-air batteries[J]. Journal of Power Sources, 2021(490): 229570.

[91] Rao P, Cui P, Yang L, et al. Surface plasma-etching treatment of cobalt nanoparticles-embedded honeysuckle-like nitrogen-doped carbon nanotubes to produce high-performance catalysts for rechargeable zinc-air batteries[J]. Journal of Power Sources, 2020(453): 227858.

[92] Hu Y, Jensen J, Zhang W, et al. Hollow spheres of iron carbide nanoparticles encased in graphitic layers as oxygen reduction catalysts[J]. Angewandte Chemie International Edition, 2014, 53(14): 3675-3679.

[93] Xia H, Zhang S, Zhu X, et al. Highly efficient catalysts for oxygen reduction using well-dispersed iron carbide nanoparticles embedded in multichannel hollow nanofibers[J]. Journal of Materials Chemistry A, 2020, 8(35): 18125-18131.

[94] Lee J, Park G, Kim S, et al. A highly efficient electrocatalyst for the oxygen reduction reaction: N-doped ketjenblack incorporated into Fe/Fe_3C-functionalized melamine foam[J]. Angewandte Chemie International Edition, 2013, 125(3): 1060-1064.

[95] Xiao Z, Wu C, Wang W, et al. Tailoring the hetero-structure of iron oxides in the framework of nitrogen doped carbon for the oxygen reduction reaction and zinc–air batteries[J]. Journal of Materials Chemistry A, 2020, 8(48): 25791-25804.

[96] Lei Y, Yang F, Xie H, et al. Biomass in situ conversion to Fe single atomic sites coupled with Fe_2O_3 clusters embedded in porous carbons for the oxygen reduction reaction[J]. Journal of Materials Chemistry A, 2020, 8(39): 20629-20636.

[97] Ma N, Jia Y, Yang X, et al. Seaweed biomass derived (Ni, Co)/CNT nanoaerogels: Efficient bifunctional electrocatalysts for oxygen evolution and reduction reactions[J]. Journal of Materials Chemistry A, 2016, 4(17): 6376-6384.

[98] Tan Y, Zhang Z, Lei Z, et al. Thiourea-zeolitic imidazolate framework-67 assembly derived Co–CoO nanoparticles encapsulated in N, S Codoped open carbon shell as bifunctional oxygen electrocatalyst for rechargeable flexible solid Zn–Air batteries[J]. Journal of Power Sources, 2020(473): 228570.

[99] Hu H, Han L, Yu M, et al. Metal–organic-framework-engaged formation of Co nanoparticle-embedded carbon@Co_9S_8 double-shelled nanocages for efficient oxygen reduction[J]. Energy & Environmental Science, 2016, 9(1): 107-111.

[100] Tian Y, Xu L, Li M, et al. Interface engineering of CoS/CoO@N-doped graphene nanocomposite for high-performance rechargeable Zn–Air batteries[J]. Nano-Micro Letters, 2020, 13(1): 3.

[101] Peng W, Yang X, Mao L, et al. ZIF-67-derived Co nanoparticles anchored in N doped hollow carbon nanofibers as bifunctional oxygen electrocatalysts[J]. Chemical Engineering Journal, 2021(407): 127157.

[102] Li P, Wang H, Fan W, et al. Salt assisted fabrication of lignin-derived Fe, N, P, S codoped porous carbon as trifunctional catalyst for Zn-air batteries and water-splitting devices[J]. Chemical Engineering Journal, 2021(421): 129704.

炭负载铁系元素催化剂在氧还原反应中的应用研究进展

李 平, 王焕磊*

（中国海洋大学 材料科学与工程学院，山东 青岛 266100）

摘 要： 金属-空气电池作为新兴的能源装置受到了人们的关注。氧还原反应 (ORR) 是金属-空气电池的关键电化学过程。由于氧还原反应缓慢的动力学速率和铂基 ORR 催化剂高昂的价格严重阻碍了金属-空气电池的规模化应用。铁系元素不但地球储量丰富而且具有多样的杂化轨道，将铁系元素引入到炭骨架中可以实现与铂相近的催化性能，非常有希望取代铂基催化剂成为商用 ORR 催化剂。本文根据活性位点的分类，对铁系元素基炭催化剂在 ORR 中的应用进行了综述，并系统总结了各中活性位点在 ORR 过程中的作用机理。本文在系统论述炭负载铁系元素催化剂结构和性能间构效关系的基础上，充分认识铁系元素在 ORR 中的作用，为今后设计具有高效 ORR 催化性能的廉价催化剂提供技术支撑和理论指导。

关键词： 铁系元素；炭基催化剂；杂原子掺杂；氧还原反应；结构调控

文章编号： 1007-8827(2021)04-0665-18 **中图分类号：** TB33 **文献标识码：** A

基金项目： 山东省自然科学基金 (ZR2020ME038)；山东省重点研发计划 (公益类科技攻关)(2019GGX102038)；中央高校基本科研业务费专项 (201941010, 201822008)；青岛市应用基础研究计划项目 (19-6-2-77-cg)；国家自然科学基金 (21471139).

通讯作者： 王焕磊，教授. E-mail: huanleiwang@ouc.edu.cn

作者简介： 李 平，博士研究生. E-mail: chemlipingest@163.com

本文的电子版全文由 Elsevier 出版社在 ScienceDirect 上出版（https://www.sciencedirect.com/journal/new-carbon-materials/）

《新型炭材料》征稿简则

《新型炭材料》创刊于 1985 年，由中国科学院主管，中国科学院山西煤炭化学研究所主办，科学出版社出版。本刊主要刊登国内外炭材料学科分支在基础科学，技术科学和与炭材料有关的边缘学科领域研究的最新成果和进展，设有研究论文、研究简报、综合评述、学术动态等栏目。

来稿要求：

1. 本刊热忱欢迎国内外学者投稿。
2. 文章录用后请上传最终版 word 文章、盖章签字的投稿推荐信和版权转让协议。
3. 投稿时请提供一张彩色主旨图和 20-30 words 的 highlights 说明。
4. 文中数据图，请采用 origin 绘图软件生成的文件，方便编辑进行编辑加工。
5. 电镜等照片，请提供层次分明的照片，最好提供单独的 JPEG 图形文件，方便编辑进行编辑加工。
6. 稿件的标题，作者姓名(所在单位、城市、邮编)、摘要、关键词、图表题、图表注、第一作者与通讯作者简介(姓名、学位、职称与 E-mail)、用中英文表示；图、表中文字一律用英文书写，图表数量小于等于 8。表格为三线或五线表。文中第一次出现缩写字时，请用写出全称。
7. 稿中的外文字母与符号须分清大、小写，正、斜体，上下角标文字符号应明显区别其高低位置。插图务求线条光洁、比例适中，照片务必清晰。
8. 中英文摘要应按照文摘四要素(目的、方法、结果、结论)进行书写。中文摘要少于 400 个汉字，英文摘要约为 1000 ~ 1500 个字符。
9. 基金资助的研究项目，请用中英文注明省部级以上基金名称和项目编号。
10. 参考文献应按文内出现顺序编号，其中“非英文参考文献”应附相应的“英文译文”。非公开的出版物请勿引用。其著录次序如下：

<期刊>［序号］作者. 文题名. 刊名，年，卷(期)：起止页码_终止页码.

例，［1］孟 亮，孙 阳，公 晗，等. 石墨烯基材料应用于水污染物治理领域的研究进展 [J]. 新型炭材料，2019，34：220-237.
(Meng L, Sun Y, Gong H, et al. Research progress of the application of graphene-based materials in the treatment of water pollutants [J]. New Carbon Materials, 2019, 34: 220-237.)

［2］Li M R, Song C, Wu Y, et al. Novel Z-scheme visible-light photocatalyst based on CoFe2O4/BiOBr/graphene composites for organic dye degradation and Cr(VI) reduction [J]. Applied Surface Science, 2019, 478: 744-753.

<图书>［序号］作者. 书名. 版次(初版不写)，出版地：出版者，年. 起止页码.

<专利>［序号］作者. 专利名称，专利号，出版日期.

<学位论文>［序号］作者. 学位论文题目，学位名称，单位名称，年份.

<论文集>［序号］析出文献作者. 析出文题名. 编者. 论文集名称. 出版地：出版者，出版年

<电子文献>［序号］作者. 文题名. 电子文献出处或可获得地址，发表或更新日期/引用日期.

对多作者文献，请注出前三个。

11. 请勿一稿多投，严禁学术不端。